GEOPHYSICAL RESEARCH LETTERS, VOL. 34, L15501, doi:10.1029/2007GL029638, 2007

Click Here for Full Article

An Antarctic ice-related "superbloom" observed with the MERIS satellite imager

Jim Gower[1] and Stephanie King[1]

Received 9 February 2007; revised 4 April 2007; accepted 9 July 2007; published 8 August 2007.

[1] MERIS (Medium Resolution Imaging Spectrometer) satellite imagery for early March 2006 shows streaks and patches of what appears to be an intense plankton bloom among broken ice off Ronne Entrance, Antarctica, near 73 S, 83 W. The streaks are 2 to 10 km wide and up to 100 km long, extending across open water between land and the ice edge. We interpret these streaks as an example of a previously reported type of "superbloom," in which very high surface concentrations of chlorophyll occur in water containing ice platelets. Spectral bands of the MERIS satellite imager in the visible and near-infrared allow computation of an index suitable for detection of surface blooms containing high concentrations of chlorophyll, especially blooms associated with high-scattering from suspended sediment or ice. The images presented here suggest a new way in which MERIS images can contribute to the study of primary productivity in polar regions. **Citation:** Gower, J., and S. King (2007), An Antarctic ice-related ''superbloom'' observed with the MERIS satellite imager, *Geophys. Res. Lett.*, *34*, L15501, doi:10.1029/2007GL029638.

1. Introduction

[2] Antarctic scientists have reported "superblooms" in which very high concentrations of algae (chlorophyll concentrations up to 200 mg.m^{-3}) occur in or near land-fast ice, close to the southern, minimum limit of ice extent [*El-Sayed*, 1971; *Sakshaug*, 1989; *Smetacek et al.*, 1992]. Blooms are most often of centric or pennate diatoms, and are associated with ice platelets in near-surface water. The diatoms appear to have bloomed in a water layer 1 to 2 meters below floating sea ice, attached to the platelets. *Smetacek et al.* [1992] suggest that the platelets have a role in anchoring the diatoms in the better-illuminated surface waters and in protecting them from grazing by zooplankton.

[3] Blooms are observed when an icebreaker penetrates the ice, or in the case of satellites, when wind opens leads and areas of open water in the ice. Observers on icebreakers commonly note the brown color of the undersides of overturned floes and ice fragments, where some algae are still attached, as well as the brown water in leads, and splashed onto surface snow [*Smetacek et al.*, 1992]. An alternative interpretation in which platelets scavenge diatoms and bring them to near-surface waters may also contribute to these blooms [*Garrison et al.*, 1983]. "Superblooms" reach higher maximum chlorophyll concentrations compared to blooms observed in the marginal ice zones, further from the poles, where melting ice promotes algae growth by stabilizing the water column [*Sullivan et al.*, 1988]. Such blooms are not associated with ice platelets.

[4] The MERIS (Medium Resolution Imaging Spectrometer) satellite imager was launched on the Envisat satellite by the European Space Agency (ESA) in March 2002. It provides images in spectral bands of visible and near infrared light with a spatial resolution of 300 m, degraded to 1200 m in standard products. MERIS spectral bands allow computation of an MCI (Maximum Chlorophyll Index) suitable for detection of surface blooms containing high concentrations of chlorophyll, especially blooms associated with a high-scattering background, such as suspended sediment or ice. The images presented here suggest a new way in which MERIS images can contribute to monitoring primary productivity in polar regions.

2. MERIS Satellite Imagery

[5] Information on the MERIS instrument on the European Space Agency's Envisat satellite is available at http://envisat.esa.int/instruments/meris/. MERIS provides continuous imagery of the earth over a swath 1150 km wide in 15 spectral bands, from a near polar orbit at an altitude of about 800 km. The center wavelengths and bandwidths of the spectral bands are chosen to define properties of water-leaving spectral reflectance and atmospheric absorption. All data shown here have a spatial resolution of 1200 m.

[6] The MCI is computed as radiance at 709 nm above a linear baseline defined by radiances at 681 and 753 nm. This shows the amplitude of a peak near 705 nm in the radiance spectrum of light reflected from the earth's surface, which several authors have associated with high surface concentrations of chlorophyll *a* in ocean, coastal and lake water targets, such as plankton blooms and floating or benthic plants [*Gitelson*, 1992; *Yacobi et al.*, 1995; *Gower et al.*, 1999].

[7] High MCI is usually caused by concentrations of chlorophyll in surface waters of 100 mg.m^3 and above, or by partly submerged vegetation [*Gower et al.*, 1999, 2005]. In both cases the peak derives from the combination of absorption by chlorophyll *a* pigment near 670 nm and water at wavelengths longer than about 720 nm, and a relatively wavelength-independent background of light scattered by suspended particles. Among satellites for monitoring large ocean and coastal areas the index is unique to MERIS, in that the band at 709 nm is not present on either MODIS or

[1]Institute of Ocean Sciences, Fisheries and Oceans Canada, Sidney, British Columbia, Canada.

Copyright 2007 by the American Geophysical Union.
0094-8276/07/2007GL029638$05.00

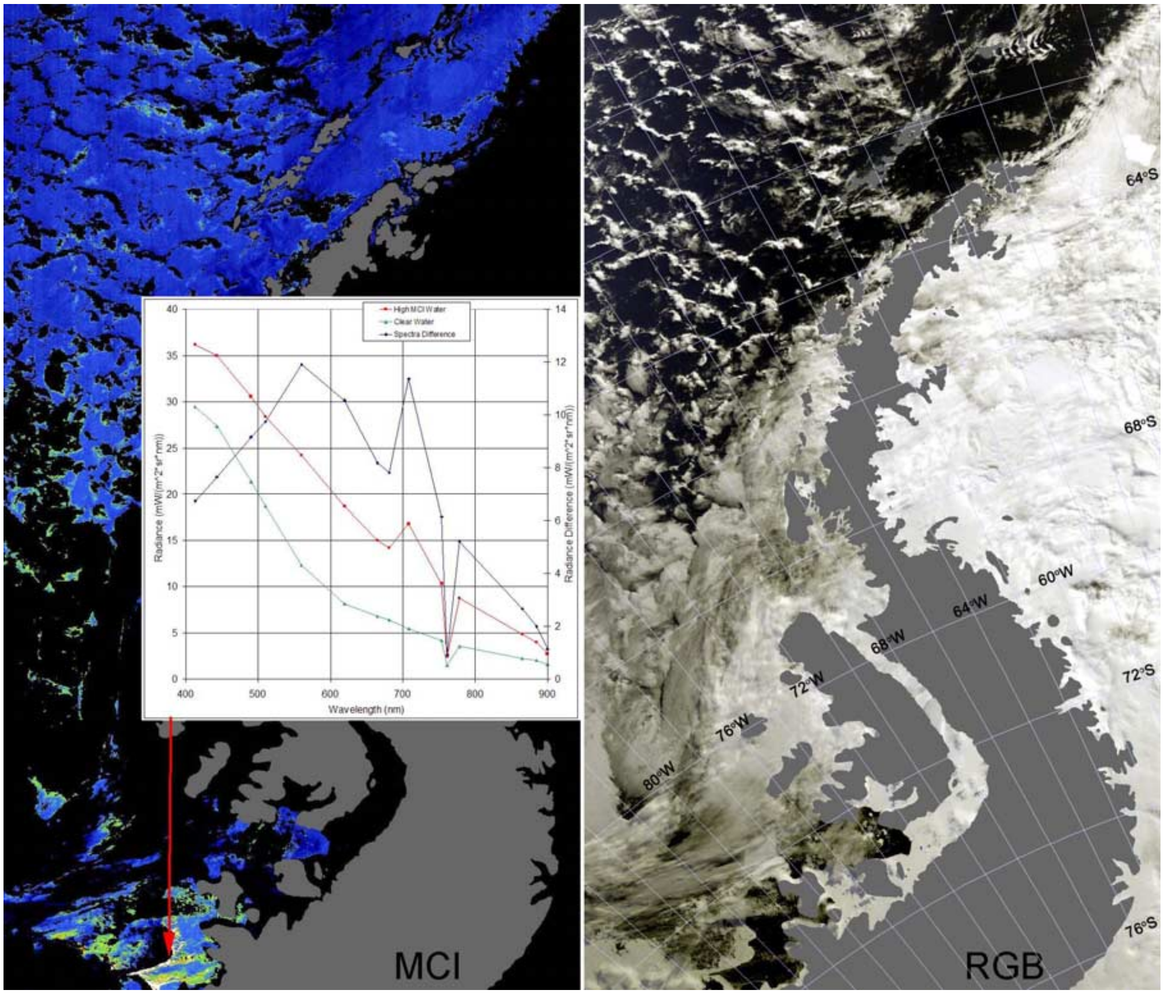

Figure 1. MERIS images of the Antarctic Peninsula on March 4 2006 with land, as mapped in a digital atlas, masked to gray. (left) MCI index image with inset showing spectra of level 1 (top of atmosphere) radiances inside (red, left axis) and outside (green, left axis) the streaks and the radiance difference (blue, right axis). Radiance in the band at 760 nm is reduced by absorption due to oxygen in the Earth's atmosphere. (right) The corresponding MERIS true color (RGB) image showing the extensive cloud and ice. Latitude and longitude lines are shown at intervals of two degrees.

SeaWiFS. Use of the MCI has also recently been demonstrated to detect and map floating *Sargassum* [*Gower et al.*, 2006].

3. MERIS Observations of This Event

[8] We have collected a limited data set of MERIS imagery of the Antarctic, and have found an example of what appears to be an intense "superbloom," observed on two dates, March 4 and March 10, 2006. We have also observed a number of less intense events in other areas on other dates. The blooms were located using the 709 nm peak MCI (Maximum Chlorophyll Index) provided by MERIS. We have no surface observations of the bloom, and base our interpretation on similarity of spatial structure to events previously reported, and on the spectra provided by MERIS, which indicate high concentrations of chlorophyll *a* in water with elevated backscatter.

[9] Values of MCI in the bloom were observed up to 4 mW/(m^2.sr.nm), which is an extremely strong signal, given that the noise level for MCI in areas unaffected by cloud, sun-glint or cosmic ray activity (impacts on the MERIS sensor) is about 0.01 mW/(m^2.sr.nm). Because of the widespread occurrence of these confusing effects, a conservative threshold for event detection would be 0.3 mW/(m^2.sr.nm), though targets with clear geometrical structure can be identified at a lower level.

[10] Figure 1 shows small cloud-free areas along the shore of the Antarctic Peninsula south of South America on March 4, 2006. In one of these areas at the Ronne Entrance near 73 S, 83 W, the MCI image (Figure 1, left), shows streaks and patches of high values. We interpret these as consisting of ice with a significant fraction of its surface covered by chlorophyll-bearing algae. The true color (RGB) image (Figure 1, right) shows the bloom to be in a small area of ice-free water surrounded by land and off-shore ice. The area is at the southern limit of MERIS data collection for this date. The limit is determined by a minimum solar elevation to ensure adequate signal for ocean optical measurements, and is unnecessarily conservative for the strong signal of the bloom.

[11] The inset graph in Figure 1 (left) shows spectra of the measured (top of atmosphere) radiance for a pixel at which MCI is high (plotted in red), for a nearby pixel at which MCI is near zero (plotted in green) and for the

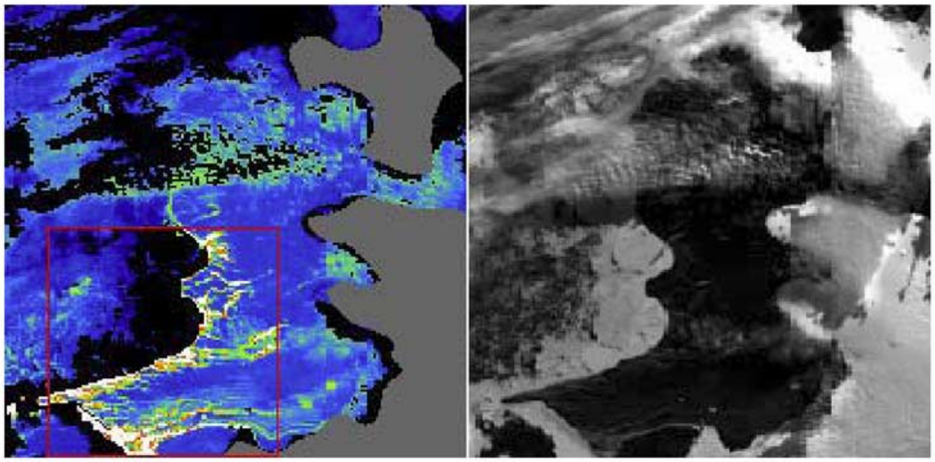

Figure 2. Enlarged area of the bloom, showing (left) MCI with land masked as before, and (right) band 6 (620 nm) radiance. The red square in Figure 2 (left) shows the area of data plotted in the scatter diagram of Figure 3.

difference between these two spectra (plotted in blue). The spectrum plotted in red has a significant peak at 709 nm, and corresponds to water colored white in the MCI image, indicating high values of this index. The spectrum plotted in green is interpreted as showing the background, "clear water" spectrum. This shows no peak, and corresponds to water colored blue in the MCI image, indicating near-zero values.

[12] The difference between these two spectra plotted in blue, shows that the "superbloom" introduces a significant radiance increase in all bands and also a prominent radiance peak at 709 nm. We interpret the broad-band increase as backscatter by ice, and the peak at 709 nm as indicating the presence of chlorophyll-bearing algae covering a significant fraction of the ice surface. The peak is due to absorption by chlorophyll *a* at wavelengths near 670 nm and absorption by water at wavelengths greater than 720 nm as described by *Gitelson* [1992], *Yacobi et al.* [1995] and *Gower et al.* [1999]. The drop in the difference spectrum (blue) at wavelengths shorter than 550 nm is also explained by chlorophyll absorption in a broad spectral band, centered near 440 nm.

[13] Figure 2 shows an enlargement of the area of the bloom in MCI and in band 6 (620 nm) of MERIS. We choose the 620 nm radiance as a measure of the average brightness of each pixel and hence, in cloud-free areas, of the average ice concentration. Some correlation is evident between unmasked areas of the left and right images. The high signals in both panels occur in patches concentrated towards the ice edge and in streaks extending in an east/west direction across the image. In these cases, areas with high MCI signal occur where ice concentration is greatest. However, the image also contains areas where band 6 radiance is high, but MCI remains low.

[14] This is more clearly seen in Figure 3 where the scatter plot (Figure 3, right), shows the range of above-

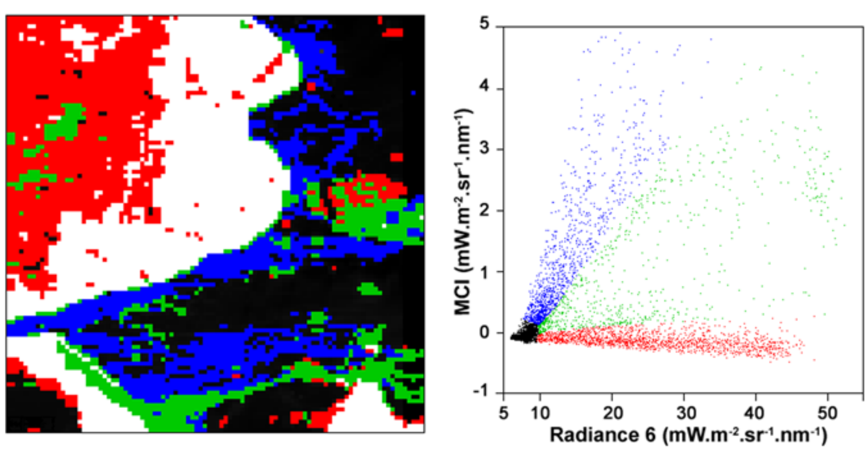

Figure 3. (left) The area of open water shown in the lower left of Figure 1 and in the red square in Figure 2, with the pixels color-coded according to the rate at which MCI increases with band 6 (620 nm) top-of-atmosphere radiance, as shown in (right) the scatter plot. The radiance at 620 nm is used as an indicator of the ice concentration in each image pixel. Red pixels show no increase in MCI with ice concentration, whereas blue pixels show a strong increase. Green pixels show an intermediate rate. White pixels indicate areas of solid or compacted ice with radiance greater than 50 mW/(m^2.sr.nm). The MCI radiance is computed as a difference from a linear baseline, and can have a negative value.

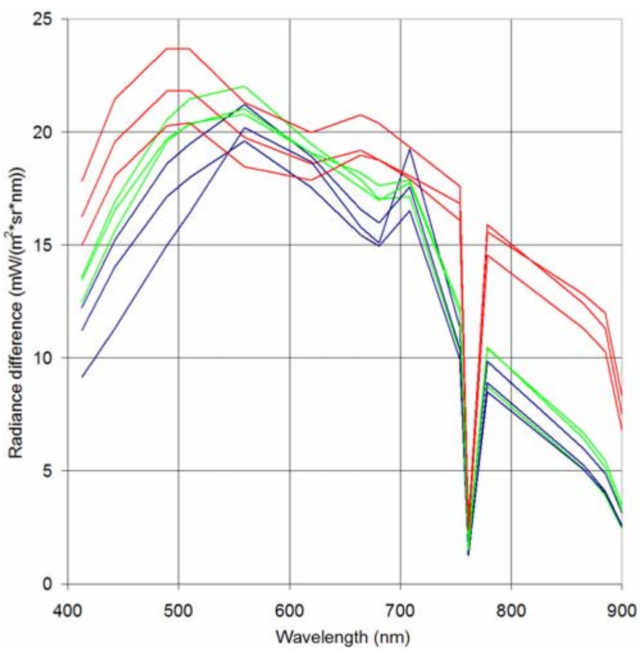

Figure 4. Spectra of the radiance increase observed between clear water and three types of ice: clean ice (red), ice with moderate algae content (green), and ice with higher algae content (blue). Colors correspond to Figure 3.

atmosphere pixel radiance at 620 nm, and the corresponding range of MCI radiance. We separate in this scatter plot, pixels showing a strong increase in MCI as 620 nm radiance (ice concentration) increases (blue), pixels showing a less-strong trend (green) and pixels showing very little or no increase in MCI (red). Pixels in which MCI and 620 nm radiances are both low, are plotted as black.

[15] Figure 3 (left) shows the spatial distribution of these pixels. Both the blue and green pixels trace out areas near the ice edge and streaks extending across the open water. We interpret these as indicating ice with algae. In contrast, we interpret the red pixels as indicating ice without algae. These pixels occur in patches rather than streaks, with a tendency to be located further from shore in the upper left of the red square in Figure 2.

[16] Figure 4 compares the spectra from representative red, green and blue pixels in Figure 3, plotted in the corresponding colors. Pixels were chosen to all have comparable radiance at 620 nm, in the range 25 to 27 mW/(m^2.sr.nm). The blue spectra show a strong peak in radiance at 709 nm, while green spectra show a weaker peak and red show none, consistent with the observed MCI values for each type of spectrum. We interpret the red spectra as showing ice with little or no phytoplankton, as suggested by absence of any relative drop in radiance near 680 nm due to absorption by chlorophyll *a*.

[17] The red spectra show higher infrared radiance than the other two types, suggesting the presence of less surface water, which would otherwise absorb this radiance. The three spectra also show evidence of absorption by chlorophyll pigments, causing lower radiance at wavelengths between 400 and 550 nm. In this wavelength range, the blue spectra show the lowest radiances, and the red the highest, as expected if absorption is due to chlorophyll *a* pigments in the algae, and is strongest for blue spectra and least for red.

4. Discussion and Conclusions

[18] Wind data from the NCEP Reanalysis Daily Average Surface Flux data set (http://www.cdc.noaa.gov/cdc/data.ncep.reanalysis.surfaceflux.html) show that winds in this area were from the east or south-east at between 5 and 10 m/s for the week preceding March 4 and continued from the east until March 10. This would drive the sea ice in Figure 2 to the west, and open up the observed area of clear water. Broken ice with the signature of high chlorophyll absorption is observed to form into narrow streaks, presumably by shear or convergence in the near-surface flow, and also to concentrate against the ice edge, as would be expected under these wind conditions.

[19] On March 10 2006, MERIS again imaged the bloom. On this date, the bloom appeared to cover a larger area, but with reduced maximum MCI signals at 709 nm, down to 2.5 mW/(m^2.sr.nm) from 4.0 mW/(m^2.sr.nm). This may indicate that the bloom event was starting to disperse, or that new ice was forming. On both dates, the bloom occurs close to the southern limit covered by the MERIS images, and appears to extend further south. The imagery also shows a number of less intense events in nearby areas on other dates.

[20] Satellite images from NASA's MODIS sensor on the Aqua and Terra satellites also show the open water where this event occurred. Images on http://rapidfire.sci.gsfc.nasa.gov/ provide higher spatial resolution and give more frequent coverage than MERIS. They confirm the presence of ice streaks and patches, but the high resolution MODIS data lack the spectral information provided by MERIS, and the full MODIS spectral band set omits the 709 band used by the MCI algorithm. MODIS images on March 4 extend further south and show that the open water extends only a short distance beyond the MERIS coverage. Other MODIS images show the ice moving offshore in January and February to form the open water in Figure 2, and the open water starting to freeze over by March 10.

[21] We present these observations in the hope that observers in the Antarctic may be able to confirm an event in or near this area at this time, or provide information on other similar events which can then be searched for in the MERIS database. Although we have no surface observations at the times of the satellite imagery, we believe that observed spatial pattern of the bloom and the spectral information provided by MERIS, give strong support to the "superbloom" interpretation. We note that the MCI index provides a useful way of detecting the events in the presence of partial cloud and ice cover, and without the need for full processing of the images. Such processing is difficult or impossible in the presence of intense phytoplankton blooms or floating ice, both of which are present in "superbloom" events.

[22] The images presented here suggest a new way in which satellite image data can make a contribution to monitoring primary productivity in polar regions. Most present and planned satellite optical sensors lack the band near 705 nm which makes this type of observation possible.

We hope that at least one instrument in the next generation of ocean color sensors will maintain this capability.

[23] **Acknowledgments.** This work was supported by Fisheries and Oceans Canada and by the Canadian Space Agency (CSA) under the GRIP (Government Related Initiative Program). Satellite imagery was provided by ESA under the Announcement of Opportunity (AO) program for scientific research applications of MERIS imagery. The authors are grateful to G. Tarling, V. Smetacek, and H. Melling for useful comments and suggestions.

References

El-Sayed, S. Z. (1971), Observations on phytoplankton bloom in the Weddell Sea, in *Biology of the Antarctic Seas*, vol. IV, *Antarct. Res. Ser.*, vol. 17, edited by G. A. Llano and J. E. Wallen, pp. 301–312, AGU, Washington, D. C.

Garrison, D. L., S. F. Ackley, and K. R. Buck (1983), A physical mechanism for establishing algal populations in frazil ice, *Nature*, *327*, 363–365.

Gitelson, A. (1992), The peak near 700 nm on radiance spectra of algae and water: Relationships of its magnitude and position with chlorophyll concentration, *Int. J. Remote Sens.*, *13*, 3367–3373.

Gower, J. F. R., R. Doerffer, and G. A. Borstad (1999), Interpretation of the 685 nm peak in water-leaving radiance spectra in terms of fluorescence, absorption and scattering, and its observation by MERIS, *Int. J. Remote Sens.*, *20*, 1771–1786.

Gower, J. F. R., S. King, G. A. Borstad, and L. Brown (2005), Detection of intense plankton blooms using the 709 nm band of the MERIS imaging spectrometer, *Int. J. Remote Sens.*, *26*, 2005–2012.

Gower, J. F. R., C. Hu, G. Borstad, and S. King (2006), Ocean color satellites show extensive lines of floating *Sargassum* in the Gulf of Mexico, *IEEE Trans. Geosci. Remote Sens.*, *44*, 3619–3625.

Sakshaug, E. (1989), The physiological ecology of polar phytoplankton, in *Marine Living Systems of the Far North*, edited by L. Rey and V. Alexander, pp. 61–89, E. J. Brill, Leiden, Netherlands.

Smetacek, V., R. Scharek, L. I. Gordon, H. Eicken, E. Fahrbach, G. Rohardt, and S. Moore (1992), Early Spring phytoplankton blooms in ice platelet layers of the southern Weddell Sea, Antarctica, *Deep Sea Res., Part I*, *39*, 153–168.

Sullivan, C. W., C. R. McClain, J. C. Comiso, and W. O. J. Smith (1988), Phytoplankton standing crops within an Antarctic ice edge assessed by satellite remote sensing, *J. Geophys. Res.*, *93*, 12,487–12,498.

Yacobi, Y. Z., A. Gitelson, and M. Mayo (1995), Remote sensing of chlorophyll in Lake Kinneret using high spectra resolution radiometer and Landsat TM: Spectral features of reflectance and algorithm development, *J. Plankton Res.*, *17*, 2155–2173.

J. Gower and S. King, Institute of Ocean Sciences, Fisheries and Oceans Canada, P.O. Box 6000, Sidney, BC, Canada V8L 4B2. (gowerj@pac.dfo-mpo.gc.ca)